Current Biology, Volume *24*

Supplemental Information

Sexually Dimorphic Octopaminergic Neurons Modulate Female Postmating Behaviors in *Drosophila*

Carolina Rezával, Tetsuya Nojima, Megan C. Neville, Andrew C. Lin, and Stephen F. Goodwin

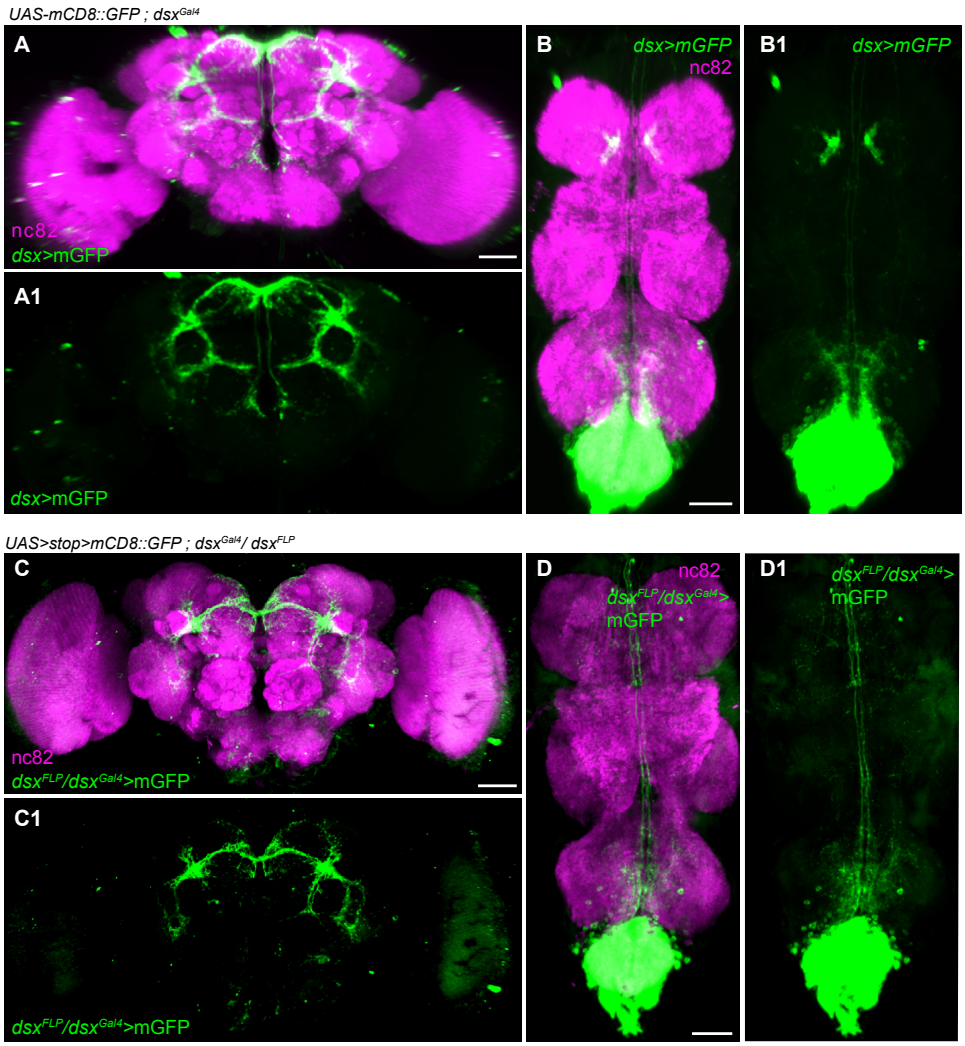

Figure S1, related to experimental procedures. Characterization of *dsx*^{FLP} neurons and associated projections.

(A-B) *dsx*^{Gal4}-neurons and associated projections in the adult female central nervous system. Expression of mCD8::GFP under the control of *dsx*^{Gal4} (*dsx*>mGFP; green) in the female brain (A) and VNC (B). (C-D) Functionality of *dsx*^{FLP} was confirmed by combining *dsx*^{FLP} with *dsx*^{Gal4} and the *UAS>stop>mCD8::GFP* reporter line. Visualization of *dsx*^{FLP}/*dsx*$^{Gal4+}$ cell bodies and projections (*dsx*^{FLP}/*dsx*^{Gal4}>mGFP; green) in the female brain (C) and VNC (D). *dsx*^{FLP} combined with *dsx*^{Gal4} and *UAS>stop>mCD8::GFP* largely recapitulates the expression pattern obtained from crossing *dsx*^{Gal4} with *UAS-mCD8::GFP.* Gustatory sensory axons do not appear to express the reporter transgene in the VNC**.** Similar results were obtained when *dsx*^{FLP} was combined with *elav*^{Gal4} and *UAS>stop>mCD8::GFP* (data not shown). Neuropil is counterstained with anti-nC82 (magenta). Scale bars: 50 µm.

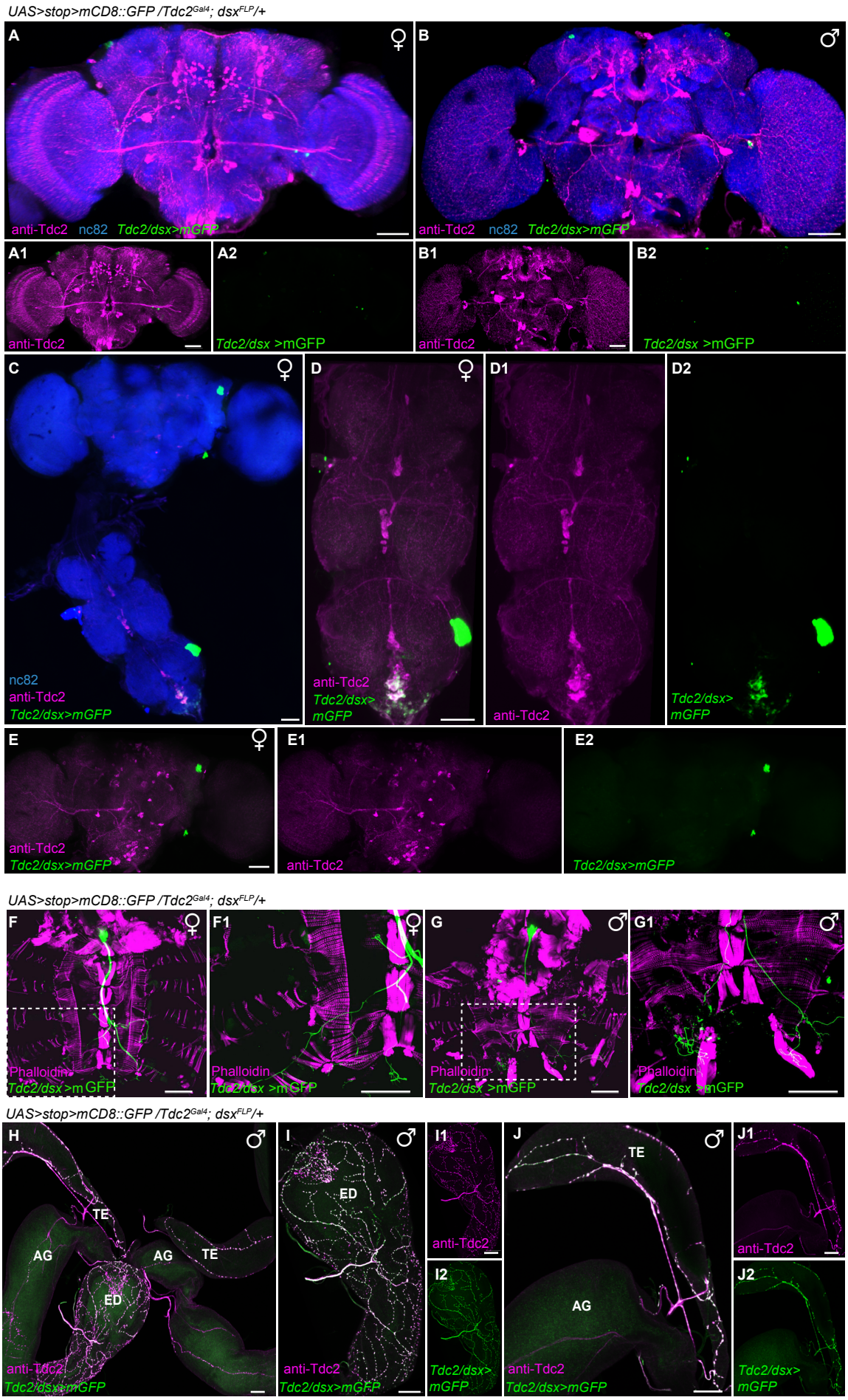
UAS>stop>mCD8::GFP /Tdc2Gal4; dsxFLP/+
A
anti-Tdc2 nc82 Tdc2/dsx>mGFP
B
anti-Tdc2 nc82 Tdc2/dsx>mGFP
A1
anti-Tdc2
A2
Tdc2/dsx >mGFP
B1
anti-Tdc2
B2
Tdc2/dsx >mGFP
C
nc82
anti-Tdc2
Tdc2/dsx>mGFP
D
anti-Tdc2
Tdc2/dsx>
mGFP
D1
anti-Tdc2
D2
Tdc2/dsx>
mGFP
E
anti-Tdc2
Tdc2/dsx>mGFP
E1
anti-Tdc2
E2
Tdc2/dsx>mGFP
UAS>stop>mCD8::GFP /Tdc2Gal4; dsxFLP/+
F
Phalloidin
Tdc2/dsx>mGFP
F1
Phalloidin
Tdc2/dsx >mGFP
G
Phalloidin
Tdc2/dsx >mGFP
G1
Phalloidin
Tdc2/dsx >mGFP
UAS>stop>mCD8::GFP /Tdc2Gal4; dsxFLP/+
H
TE
AG
AG
TE
ED
anti-Tdc2
Tdc2/dsx>mGFP
I
ED
anti-Tdc2
Tdc2/dsx>mGFP
I1
anti-Tdc2
I2
Tdc2/dsx>
mGFP
J
TE
AG
anti-Tdc2
Tdc2/dsx>mGFP
J1
anti-Tdc2
J2
Tdc2/dsx>
mGFP

Figure S2, related to Figure 3. Characterization of *dsx*/*Tdc2*$^{+}$ neurons and associated projections.

(A-J) Combining the *dsx*^{FLP} line with *Tdc2-Gal4* allows expression of *UAS>stop>mCD8::GFP* in *Tdc2/dsx*$^{+}$ co-expressing neurons (*Tdc2*/*dsx*>mGFP; green). Visualization of *Tdc2*/*dsx*$^{+}$ neurons in the adult female (A) and male brain (B). Neither the female or male brain shows mGFP expression. (C-E) Female brain and VNC of a single preparation showing *Tdc2/dsx*>mGFP neurons (green). Higher magnification of the female VNC (D) and brain (E) showing that *dsx/Tdc2*$^{+}$ overlap is restricted to a small subset of neurons within the female Abg. (A-E) Anti-Tdc2 staining is shown in magenta. Neuropil is counterstained with anti-nC82 (blue). Scale bars: 50 µm. (F-G) Visualization of *Tdc2*/*dsx*$^{+}$ neuronal projections in the female (F) or male (G) adult abdominal muscles (*Tdc2/dsx*>mGFP*;* green). Phalloidin is shown in magenta. Scale bars: 200 µm. (H-J) Visualization of *Tdc2*/*dsx*$^{+}$ neuronal projections in the male reproductive system (*Tdc2/dsx*>mGFP*;* green). Anti-Tdc2 staining is shown in magenta. The ejaculatory duct (ED), accessory gland (AG) and testes (TE) are shown at higher magnification (I and J, respectively). Scale bars: 25 µm.

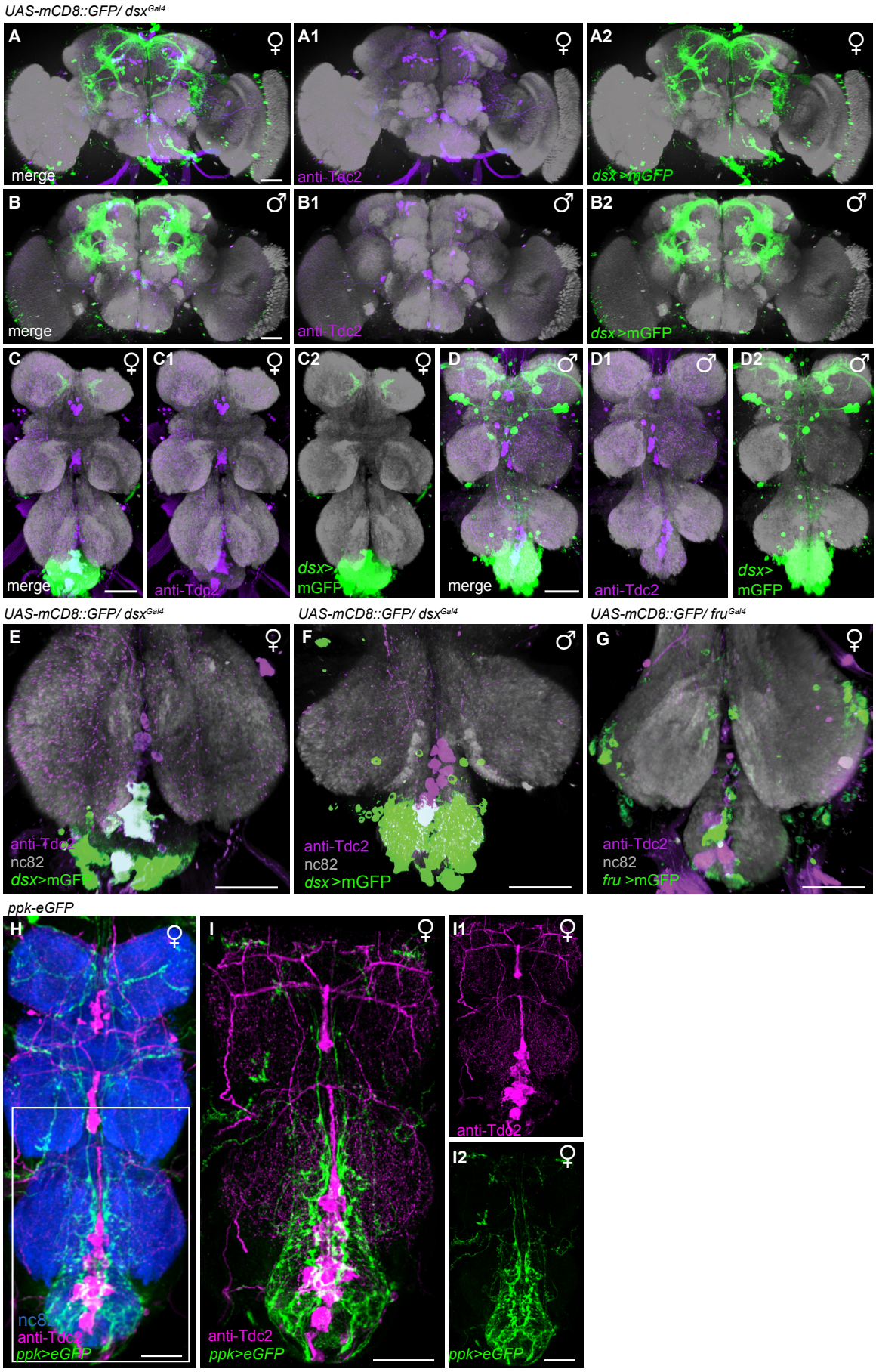
UAS-mCD8::GFP/ dsx^Gal4
A
merge
A1
anti-Tdc2
A2
dsx >mGFP
B
merge
B1
anti-Tdc2
B2
dsx >mGFP
C
merge
C1
anti-Tdc2
C2
dsx>
mGFP
D
merge
D1
anti-Tdc2
D2
dsx>
mGFP
UAS-mCD8::GFP/ dsx^Gal4
E
anti-Tdc2
nc82
dsx>mGFP
UAS-mCD8::GFP/ dsx^Gal4
F
anti-Tdc2
nc82
dsx >mGFP
UAS-mCD8::GFP/ fru^Gal4
G
anti-Tdc2
nc82
fru >mGFP
ppk-eGFP
H
nc82
anti-Tdc2
ppk>eGFP
I
anti-Tdc2
ppk>eGFP
I1
anti-Tdc2
I2
ppk>eGFP

Figure S3, related to Figure 3. *Tdc2*$^{+}$ expression analyses with *dsx*^{Gal4}, *fru*^{Gal4} and *ppk-eGFP*.

Expression of mGFP under the control of *dsx*^{Gal4} (*dsx*>mGFP; green) in the female and male brain (A and B, respectively) and female and male VNC (C and D, respectively). Higher magnification of the female and male Abg depicting co-localization between *dsx*^{Gal4} and *Tdc2*$^{+}$ neurons (labeled with Anti-Tdc2; E and F, respectively). (G) Expression of mGFP under the control of *fru*^{Gal4} (*fru*>mGFP; green) in the female Abg. No *Tdc2*$^{+}$ neurons co-express *fru*^{Gal4} in the female Abg (G) or male Abg [S1].(A-G) Anti-Tdc2 staining is shown in magenta. Neuropil is counterstained with anti-nC82 (grey). Scale bars: 50 µm. (H,I) *ppk*-eGFP labels *ppk* cell bodies and processes (*ppk*>GFP; green), while *Tdc2*$^{+}$ neurons are visualized with anti-Tdc2 antibody (magenta) in the adult female VNC. (I) Higher magnification of white box in (H) shows no overlap between *ppk* and *Tdc2*$^{+}$ cell bodies in the Abg.

Supplemental Experimental Procedures

D. melanogaster strains and crosses

All flies were raised at 25°C on standard medium in a 12 hr light /12 hr dark cycle. Wild-type flies were obtained from a *Canton-S* strain. We obtained the *UAS-mCD8::GFP*, *Tdc2-Gal4, UAS-Tdc2 RNAi* (TRiP) lines from Bloomington *Drosophila* Stock Center. Other fly stocks used were dsx^{Gal4} [S2], and fru^{Gal4}, *UAS>stop>mCD8::GFP*, *UAS>stop>LacZ*, *UAS>stop>TNT*, $UAS>stop>trpA1^{myc}$ (provided by B. Dickson), *UAS>stop>myrGFP* (provided by G. Rubin), $t\beta h^{nM18}$ (provided by M. Monastirioti), $Tdc2^{R054}$ (provided by J.Hirsh), $UAS\text{-}TNT_G$ (provided by S. Sweeney), *UAS-TrpA1* (provided by P. Garrity) and *ppk-eGFP* (provided by W.B Grueber).

Targeted insertion of FLP into the *dsx* locus.

FLP was targeted to the *dsx* locus by ends-in homologous recombination [S3]. The dsx^{FLP} allele was generated as previously described for dsx^{Gal4} [S2]; however, Gal4 was replaced by FLP using BamHI (5') and MluI (3') restriction sites. The coding sequence of FLP was codon optimised using the GeneOptimizer software, and synthetized by GeneArt (Life Technologies). dsx^{FLP} is not a *dsx* null mutant; dsx^{FLP} homocigotes are fertile and show normal morphology (data not shown).

Immunohistochemistry

Flies were reared at 25°C and aged for 4–6 days (for nervous system) or for 7-10 days (for reproductive system) prior to dissection and staining as previously described [S1, S4]. Primary antibodies used were: rabbit anti-GFP (1:1000,

Invitrogen Molecular Probes, Carlsbad, CA), chicken anti-GFP (1:1000, Abcam), mouse mAb nC82 (1:10, DSHB, Univ. of Iowa, IA), and rat anti-ELAV (1:500, DSHB, Univ. of Iowa, IA), rabbit anti-βGal (1:1000; Cappel, ICN). Secondary antibodies used were: anti-rat Cy5, anti-rabbit Alexa Fluor488, and anti-mouse Alexa Fluor546 conjugates (1:300 Invitrogen Molecular Probes, Carlsbad, CA) and anti-chicken Alexa Fluor488 (1:500 Invitrogen Molecular Probes, Carlsbad, CA). Phalloidin-546 (Sigma) was used at a dilution of 1:500 for 2 hr. Confocal stacks were taken with Olympus FV1000 and Leica SP5 microscopes. Images were processed in Amira 5.2 (Mercury Systems).

Behavioral assays

All behavioral experiments were carried out at 25°C. *Percentage copulation*: individual 3-5 day old virgin females were introduced into a round courtship chamber (19 mm diameter × 4 mm height) with an individual naïve *Canton-S* male. The percent of females achieving copulation within 1 hr was measured. *Latency to copulation*: time elapsed between introduction of females and copulation. *Male courtship index*: percentage of time during which a male displays any of the courtship steps, including following, tapping, wing extension, licking, and attempted copulation. O*vipositor extrusion:* number of ovipositor extrusions performed by the female per minute during the observation period of courtship. Courtship index and ovipositor extrusion were measured during a 3 min observation period (or until mating occurred) starting from the time of courtship initiation). *Remating*: percentage copulation was measured for 1 hour using the same mated females 48 hr after copulation. *Egg-laying*: individual 4–5 day old females were transferred to a fresh vial with media and allowed to lay eggs for 48 hr at 25°C. For thermal activation experiments, individual females were introduced into a round courtship chamber (10 mm diameter × 4 mm

height) with an individual naïve *Canton-S* male, which was then placed on a heating plate (*Techne Dri-block heater*). Experiments were performed either at 22°C or 31°C. For *octopamine feeding* experiments*,* newly eclosed virgin females were aged for 6 d in vials with Instant *Drosophila* medium (Carolina Biological Supply Company) containing 7.5 mg/mL of octopamine (Sigma) and 0.25 mg/mL Indigo Carmine and tested for the indicated behaviors.

Statistics

Behavioral means were compared using Kruskal-Wallis ANOVA test and Dunn's post hoc statistical test where indicated. For Fisher's exact test, two-tail *p* values were compared with controls. Statistical analyses were performed with GraphPad Prism software (version 6.0b, SPSS Inc.).

Supplemental references

S1. Nojima, T., Kimura, K., Koganezawa, M., and Yamamoto, D. (2010). Neuronal synaptic outputs determine the sexual fate of postsynaptic targets. Curr Biol *20*, 836-840.

S2. Rideout, E.J., Dornan, A.J., Neville, M.C., Eadie, S., and Goodwin, S.F. (2010). Control of sexual differentiation and behavior by the doublesex gene in Drosophila melanogaster. Nat Neurosci *13*, 458-466.

S3. Rong, Y.S., and Golic, K.G. (2000). Gene targeting by homologous recombination in Drosophila. Science *288*, 2013-2018.

S4. Billeter, J.C., Villella, A., Allendorfer, J.B., Dornan, A.J., Richardson, M., Gailey, D.A., and Goodwin, S.F. (2006). Isoform-specific control of male neuronal differentiation and behavior in Drosophila by the fruitless gene. Curr Biol *16*, 1063-1076.